Status of the HMPID CsI-RICH Project for ALICE at the CERN/LHC

A. Di Mauro, Y. Andres, B. Belin, A. Braem, K. Chileev, M. Davenport, G. De Cataldo, D. Di Bari, A. Franco, U. Fratino, A. Gallas, F. Guber, H. Hoedlmoser, A. Kurepin, P. Martinengo, E. Nappi, G. Paic, C. Pastore, F. Piuz, J. C. Santiard, E. Schyns, I. Sgura, and A. Tauro

***Abstract*—The ALICE (A Large Ion Collider Experiment) high momentum particle identification (HMPID) detector, presently under construction, consists of seven identical proximity focusing ring imaging Cherenkov (RICH) counters exploiting large area CsI photocathodes for Cherenkov light imaging. With a total area of 11 m^2, it represents the largest CsI-RICH system ever used in High Energy Physics. The detector layout, assembly and quality checks will be presented, with particular emphasis on CsI photocathodes mass production. A validation procedure has been established combining the results of the photocathode response mapping obtained in a dedicated VUV scanner with test beam data. The long-term stability has also been studied by irradiation with a Sr-90 source of a final size CsI photocathode inside a detector prototype.**

***Index Terms*—Ageing, Cherenkov detectors, CsI, photocathodes, quantum efficiency.**

I. Introduction

ALICE (A Large Ion Collider Experiment) is a general purpose heavy-ion experiment, specifically optimized to study Pb-Pb collisions at the CERN/LHC, at a center of mass energy per nucleon pair of $\sqrt{s_{NN}} = 5.5$ TeV with a luminosity of $10^{27}\ \mathrm{cm}^{-2}\mathrm{s}^{-1}$ [1]. Head-on collisions between ultra-relativistic heavy ions are expected to provide the conditions of energy densities corresponding to the phase transition of hadronic matter to a state where quarks are no longer confined within the nucleus (quark-gluon plasma). Interactions between lower mass nuclei, p-A and p-p, will also be studied as benchmark and reference data for heavy-ion physics. ALICE will address both hadronic and leptonic signals in a wide momentum range, from 100 MeV/c to 100 GeV/c, up to the largest anticipated charged particle density of 8000 per unit of rapidity in central Pb-Pb collisions. Particle identification (PID) plays a key role in the characterization of such events. Therefore, a complex PID scheme has been implemented, with four central detectors covering the full ALICE barrel: the inner tracking system (ITS), the TPC, the transition radiation detector (TRD), and the time-of-flight (TOF). In addition, a single-arm detector, the high momentum PID (HMPID), is devoted to the identification of high transverse momentum p_T charged hadrons.

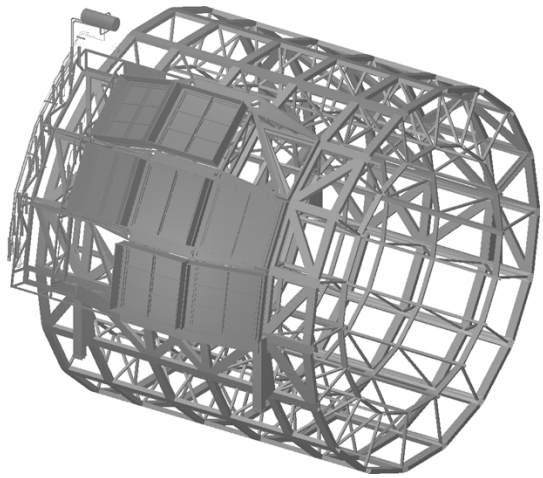

Fig. 1. Drawing of the ALICE space frame with the HMPID support cradle and seven detector modules.

The HMPID system consists of an array of seven identical ring imaging Cherenkov (RICH) detector modules of 1.5 m × 1.5 m, located at a radial distance of 4.7 m from the interaction point and covering 5% of the central barrel phase space (Fig. 1) [2]. Each module is equipped with six CsI photocathodes (PCs) of 0.64 m × 0.4 m, thus resulting in a total active area of 11 m^2. The detector has been designed to identify pions and kaons in the range $1 \leq p \leq 3\ \mathrm{GeV/c}$ and protons in the range $2 \leq p \leq 5\ \mathrm{GeV/c}$, with the largest anticipated charged particles multiplicity of $100\ \mathrm{m}^{-2}$. The detector size and the adopted layout are dictated mainly by physics requirements [1], [2]. The measurement of correlations between high p_T particles, giving information on the size of the emitting source, imposes a minimum detector size both in the beam direction and in the azimuthal angle coverage. Besides, the module orientation with respect to the interaction point, minimizes the dip angle of incoming particles to within 10° of normal incidence. As a result, Cherenkov rings deviations from the circular shape are kept within limits optimized for an efficient pattern recognition [2].

Manuscript received December 1, 2004; revised April 29, 2005.

A. Di Mauro, Y. Andres, A. Braem, M. Davenport, G. De Cataldo, A. Gallas, H. Hoedlmoser, P. Martinengo, F. Piuz, J. C. Santiard, and E. Schyns are with CERN, the European Laboratory for Particle Physics, 1211 Genève 23, Switzerland (e-mail: Antonio.Di.Mauro@cern.ch).

B. Belin is with Tubitak, Istanbul Technical University, Istanbul 34469, Turkey.

K. Chileev, A. Franco, E. Nappi, C. Pastore, I. Sgura and A. Tauro are with the Istituto Nazionale di Fisica Nucleare (I.N.F.N.), 70121 Bari, Italy.

D. Di Bari is with the Dipartimento Interateneo di Fisica, Università degli Studi, 70121 Bari, Italy.

U. Fratino is with the Politecnico di Bari, 70121 Bari, Italy.

F. Guber and A. Kurepin are with the Institute for Nuclear Research (INR), 141980 Moscow, Russia.

G. Paic is with the Instituto de Ciencias Nucleares (UNAM), 04510 Mexico DF, Mexico.

Digital Object Identifier 10.1109/TNS.2005.852743

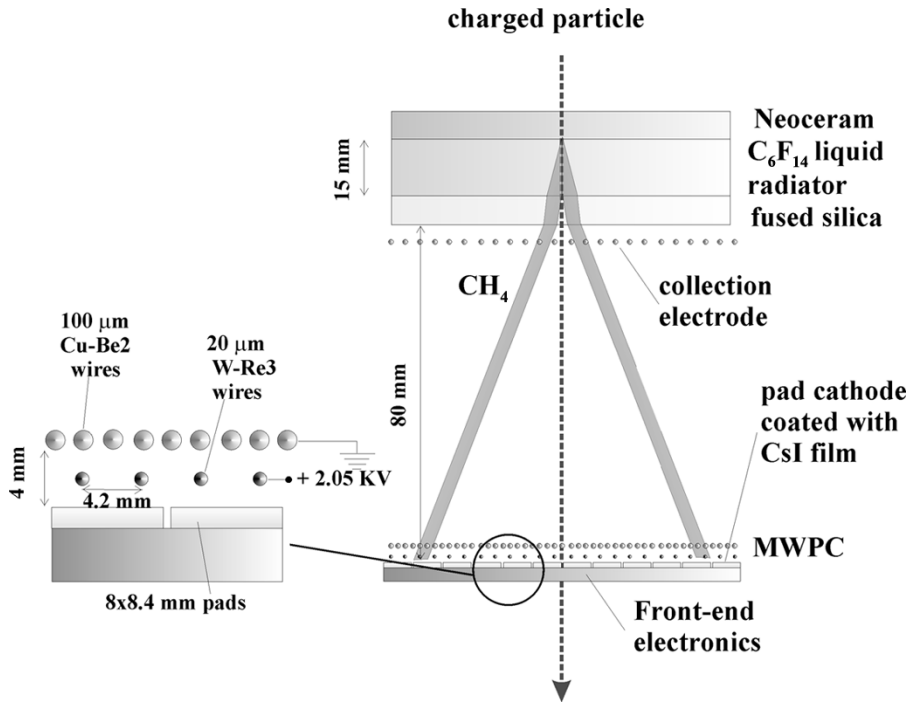

Fig. 2. Schematic cross section of the HMPID RICH detector.

Like all detectors involved in LHC experiments, the HMPID system is presently under construction. Although many requirements, corresponding to an optimal and stable PID performance, have to be fulfilled at the level of detector design and assembly, the production and validation of the needed 42 CsI PCs represent the most challenging part of the project.

After a description of the detector layout and assembly, the studies performed to establish the validation procedure for the CsI PC serial production will be presented. Finally, the results of ageing tests, pointing out a possible *self-ageing* mechanism, will be discussed.

II. Detector Layout

A detailed description of the ALICE HMPID RICH can be found in [2], [3]. The detector schematic cross section is shown in Fig. 2. The RICH has a proximity focusing configuration, with a 15-mm-thick layer of C_6F_{14} (perfluoro-hexane) liquid radiator circulated in vessels having 5-mm fused silica windows, nearly transparent to the Cherenkov radiation of interest (Fig. 3). The C_6F_{14} refractive index at $\lambda = 175$ nm is $n = 1.2989$, corresponding to $\beta_{\min} = 0.77$, namely a threshold momentum $p_{th} = 1.21\ m$ GeV/c, with m equal to the particle mass in GeV/c^2.

The Cherenkov light produced in the fused silica window is internally reflected and does not escape the window itself, provided the particle incidence angle is smaller than $\sim 12°$. Only low momentum particles, below ~1 GeV/c, will have larger incidence angles and the corresponding Cherenkov light produced in the quartz will contribute to the background noise.

The photon detector is an open geometry MWPC operated with CH_4 at atmospheric pressure; it has one cathode plane segmented into 80 × 48 pads of 8 mm × 8.4 mm and coated with a 300-nm photosensitive layer of CsI. An additional wire plane positively biased, located just after the quartz window, acts as collection electrode to prevent electrons released by charged particles in the proximity gap entering the 4-mm sensitive gap.

Fig. 3. The three radiator vessels equipping one HMPID module.

The readout of the HMPID modules, having in total 161 280 pads, is organized according to a parallel/serial architecture and is based on two ASICs specifically developed for this application: the GASSIPLEX chip [4], a 16-channels charge sensitive pre-amplifier and shaper, enabling the determination of the hit coordinates by centroid measurement, and the DILOGIC chip [2], a digital processor for zero suppression. The GASSIPLEX is characterized by a filtering scheme designed to cope with the shape of the signal delivered by MWPCs and by a long peaking time (1.2 μs) suitable for an external event trigger. An average noise of 1000 e^- per channel has been measured on detector.

The gas and liquid circulation systems have been designed to fulfill the requirements of high purity of the fluids and safe operation.

High gas purity (5 ppm of O_2 and H_2O) is required by the large CsI hygroscopicity (exposure to moisture can damage the PC and result in a QE deterioration). Assembly materials and system component have been selected to ensure total absence of silicon and other outgassed pollutants for the stability of the MWPC efficiency.

The chamber deformation induced by the gas pressure has to be minimized to keep the parallelism of radiator vessels and PCs within 200 μm and avoid the breaking of the fragile radiator vessels resulting from the deflection of the supporting composite panel. A module has a total volume of 200 L and can be flushed up to 100 L/h with Ar, during stand-by, or CH_4, during operation. The gas pressure will be kept at 2–3 mbar and a no-return mechanical safety valve, calibrated at 10 mbar, isolates the chambers from exhaust bubblers, filled with FomblinZ25 (Solvay-Solexis, www.solvaysolexis.com), a perfluoro-polyether lubricant characterized by an extremely low vapor pressure (5×10^{-12} torr at 20°C).

The liquid circulation system has to fill and drain the radiator vessels (of 8 L volume each) independently, remotely and safely, at a constant flow of 4 L/h. Given its intrinsic high degree of safety, gravity flow has been adopted to prevent accidental large hydrostatic loads in the fragile radiator vessels [2], [5]. In addition, C_6F_{14} has a high affinity for O_2 and H_2O resulting in a decrease of the transparency in the VUV region, the Cherenkov photons spectral range where CsI is sensitive (photoelectric threshold ~6.2 eV). Therefore, a dedicated filtering station will be implemented.

The front-end and read-out electronics are enclosed in a tight box on the backside of the module, flushed with nitrogen and closed by a heat screen panel. The power consumption amounts to about 400 W per module and the corresponding heat will be removed by a cooling system circulating water through the heat screen, composed by two stainless steel thin plates welded together and shaped to allow water flow over the full surface.

III. Status of the Production

The HMPID modules production is divided into four main lines: the MWPC, the radiator vessels, the CsI PCs, the front-end electronics (FEE).

Five out of seven chambers including the MWPC and the radiator vessels have been completed and commissioned in the laboratory and test beam.

The mass production of 42 CsI PCs started in May'04, and 17 have been used to equip Module-2, Module-3 and Module-4 for the commissioning in test beam. Module-1 has been checked in the test beam in 2003 using pre-series CsI PCs.

All the chips needed for the FEE, the 10 080 GASSIPLEX and 3360 DILOGIC chips, have been mounted on cards and tested.

IV. Detector Assembly and Quality Checks

Each module is equipped with three radiator vessels of 1330 mm × 413 mm × 24 mm, made of NEOCERAM, a transparent ceramic having thermal coefficient very close to the fused silica plates used as UV-transparent windows (Fig. 3). Three rows of ten fused silica rods are glued between the NEOCERAM bottom plate and the fused silica windows to achieve the necessary strength to withstand the hydrostatic load. The radiator support is a composite panel, obtained by sandwiching two 0.5-mm Al foils with a 50-mm plate of ROHACELL-51, a rigid and very light foam (0.0513 g/cm^3), to minimize the radiation length of the detector "entrance window". The vessels are He-leak tested both after the assembly gluing and after the mounting on the support.

The MWPC is a stack of four Al frames of 1.5 m × 1.5 m, holding the different wire planes, machined with a planarity of 0.1 mm; the same accuracy is achieved in the sensitive gap and in the positioning of radiators with respect to the PCs. Such a stack is closed on one side by the radiator panel support and on the other side by the CsI PCs; Viton O-rings are inserted between the frames to form a leak tight vessel. The nominal gap between the anode and the PC is 2 mm. The 20 μm gold plated W-Re anode wires are soldered on a G10 printed circuit board with a pitch of 4.2 mm and a precision of 0.05 mm, at a tension of 46 ± 1 g corresponding to 70% of the wire elastic limit. Support bars of MACOR (Corning, [1]), a special glass ceramic for high precision machining, are inserted between the pad cathode and the anode plane at half length of the 130-cm wires in order to ensure the stability of the sense wires under the electrostatic force and minimize the sensitive gap variation due to wire sagging. The second cathode plane is placed at 2.45 mm from the anode plane and is obtained by stretching 100 μm gold plated Cu-Be wires, with a pitch of 2.1 mm, at a tension of 210 ± 10 g using crimping pins located in a comb-like structure fixed on the support frame. Finally, the collection electrode, placed next to the radiator vessel exit window, consists of 100 μm gold plated Cu-Be wires stretched at a tension of 55 ± 5 g, with a pitch of 5 mm.

Several quality checks are performed during and after the assembly: metrology, wire tension measurement, leak rate measurement, HV commissioning under CO_2 (having no amplification it allows to reach safely higher HV than nominal to test the wires mechanical stability under high electric field), gain mapping with a Sr-90 source under CH_4.

V. CsI Photocathodes Production

The CsI QE is affected by the choice of the substrate material and its surface quality at microscopic level, as well as by the handling following the CsI deposition. A special procedure has been established to ensure the surface quality needed to achieve high and reproducible QE [2], [6]–[8]. Fig. 4 shows the evolution of the CsI QE at 170 nm of large area PCs produced within the CERN/RD26 collaboration, up to 1997, and by the HMPID project, later on.

The PC final processing, improved by several new tests on substrate types, preparation, heat conditioning, and use of a transfer system designed to avoid exposure to air, is in use from 2000 when PC33 was produced.

Double-layer printed circuit boards (PCBs) with blind holes have been chosen to provide leak tight connections of the cathode pads to the FEE connectors on the back of the PC. The PCBs are specially prepared to act as substrate for the CsI layer.

[1]Available: www.corning.com

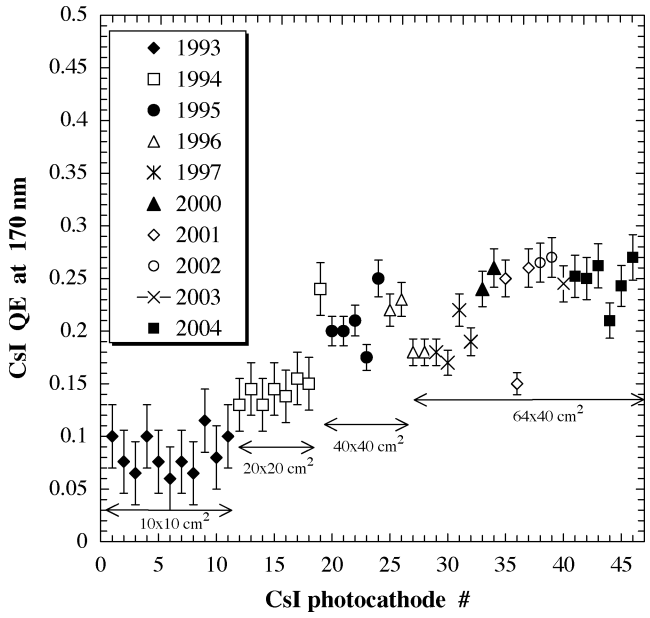

Fig. 4. Summary of the CsI QE at 170 nm of the PCs produced by the CERN/RD26 collaboration, until 1997, and by the HMPID project, later on. The PC size is also indicated under the arrows.

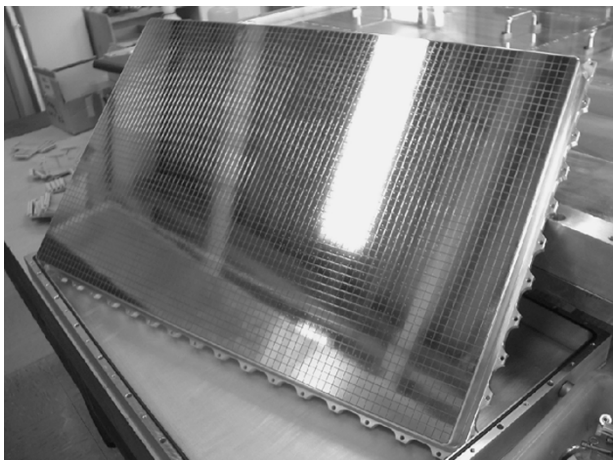

Fig. 5. A pad cathode panel (80 × 48 pads of 8 mm × 8.4 mm) before the coating with CsI. The reflection of the illuminating light enhances the mirror-like quality achieved on the PC substrate.

The Cu pads, accurately polished by chemical and mechanical treatments, are covered with a 7 μm layer of Ni and a 0.5 μm layer of Au. The first layer acts as a barrier preventing the reaction of CsI with Cu, the second was found to be suitable for CsI coating. A pad cathode panel (Fig. 5) is composed of two such PCBs glued onto a stiff Al frame (4 cm thick) using a vacuum table to achieve planarity better than 50 μm.

Pollution can occur during the many steps of the production, e.g. when the FEE connectors are mounted on the circuit. It has been found essential to apply an ultrasonic cleaning to the panel just before the coating, using strong detergents, demineralized water and pure ethylic alcohol. The pad cathode is then coated in a large deposition plant, where CsI is evaporated by the Joule effect from four molybdenum crucibles, at a substrate temperature of 60 °C and a pressure of 5×10^{-7} mbar. Residual gas analysis (RGA) is performed prior to the deposition to ensure that

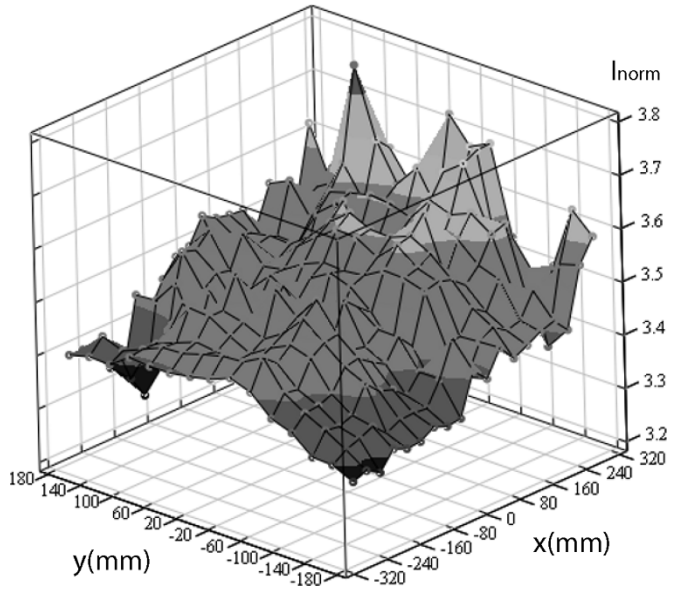

Fig. 6. The normalized photocurrent response mapping of PC45 characterized by an average of 3.5 over the full scanned area.

residual pollution is at acceptable level (in particular, $H_2O < 4 \times 10^{-4}$ ppm and hydrocarbons $C_xH_y < 5 \times 10^{-5}$ ppm).

After the CsI deposition, heat conditioning under vacuum at 60 °C for 12 h is performed to achieve the final QE. Finally, the PC is encapsulated under Ar in a sealed protective box and always kept under gas flow to avoid any exposure to moisture. Eventually it is mounted on the detector by means of a large, custom-made, glove-box that can be attached directly to the HMPID module.

VI. The VUV Scanner

Before the starting of the serial production, the PC response was evaluated only from test beam of the HMPID detector prototypes, with a procedure allowing to estimate the detector performance and the CsI QE, with the support of a Monte Carlo simulation [9]. To simplify the characterization of the large number of PCs during the mass production, a dedicated VUV scanner system has been implemented in a large vessel attached to the evaporation plant. After CsI deposition a PC is transferred under vacuum to the VUV scanner system, where the photocurrent induced by a collimated light beam from a deuterium lamp with MgF_2 window is recorded over the full photosensitive area. Such a system allows in-situ characterization of the produced PCs providing a mapping of the response to the lamp integral spectrum [3], [10]. A revolving mirror directs the light either to the PC under characterization or to a reference CsI phototube measuring the incident photon flux for normalization.

As an example, Fig. 6 shows the normalized photocurrent mapping measured on PC45, characterized by an average of 3.5 and a spread of 10% over the full area. The observed inhomogeneity has never a systematic aspect and is below 15% in all validated PCs. A summary of the average response of the 17 produced CsI PCs is reported in Fig. 7. The QE degradation after PC54 resulted from the not optimized condition during the CsI evaporation owing to the use of spare vacuum pumps.

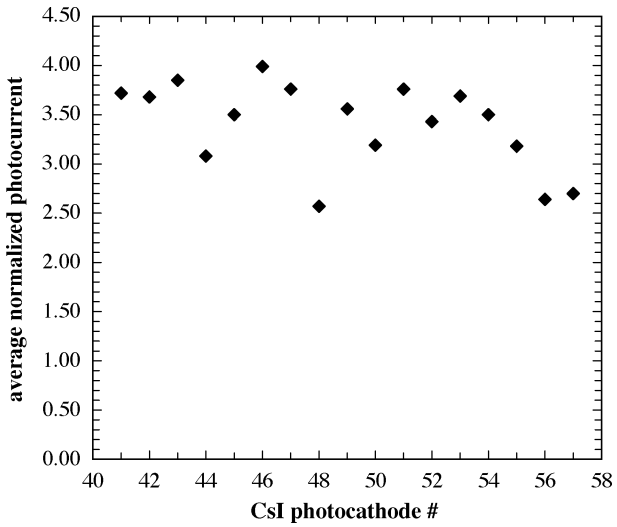

Fig. 7. Summary of the average normalized photocurrent of the first 17 CsI PCs (41 to 57) of the serial production.

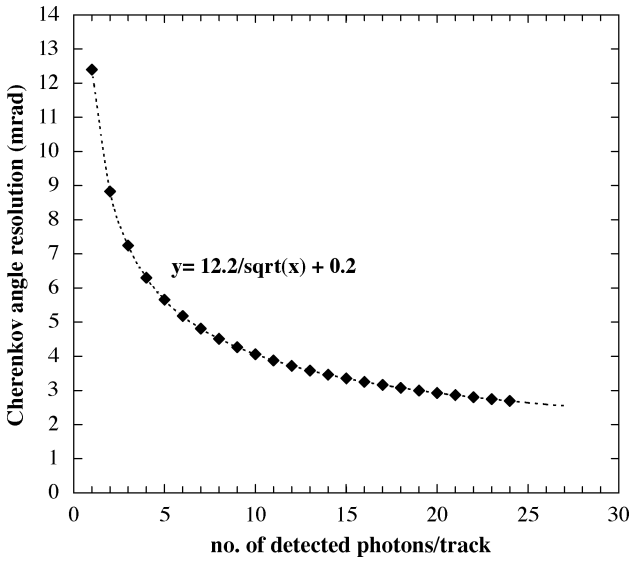

Fig. 8. Measured Cherenkov angle resolution/track as a function of the number of detected photons per track. The fitting curve indicates the dependence of the angular resolution from the inverse of the square root of the number of detected photons.

VII. Photocathodes Validation and PID Performance

Many checks have been introduced at different stages of the PC production, from the PCB manufacturing to the encapsulation in the protective box, in order to ensure as high and reproducible QE as possible. However, like in the production of commercial phototubes, variations of the CsI QE cannot be avoided, especially in such large area devices.

Although quite relevant for a correct analysis of ALICE events, the integral spectrum response mapping cannot be used alone to set a threshold for acceptance of the PCs. Given the different spectrum of the Cherenkov photons to be detected, the measured normalized photocurrent cannot be translated into detector PID performance. Hence, a validation procedure can be established only by relating VUV scanner response and test beam data.

Fig. 8 shows the variation of the Cherenkov angle resolution from single photon up to 25 detected photons, measured in single particle events from test beam of the HMPID modules produced in 2004. The fitting curve corresponds, as expected, to inverse proportionality between the angular resolution and the square root of the number of detected photons. From these results, one could deduce a π-K separation better than 4σ up to 3 GeV/c with 15 detected photons per ring. Previous studies of pattern recognition in multi-particles events have shown that, even in background conditions corresponding to the largest anticipated multiplicity of 100 m^{-2}, a 3σ π-K separation can still be achieved at 3 GeV/c with 15 detected photons [2]. Nevertheless, the threshold for PC acceptance has been set at 17 detected photons, taking into account two additional aspects, which will be further treated in the next sections.

First, the number of detected photons per ring, although mainly determined by the PC response, depends also on detector operating parameters, namely the transmission of the $\mathrm{C_6F_{14}}$ radiator to the Cherenkov radiation, and the gas gain, affected by changes in the atmospheric pressure. In steady running conditions, the $\mathrm{C_6F_{14}}$ recirculation through filters will allow reaching a high quality, while the gas gain variations with the pressure will be compensated with adjustment of the anode wires voltage. During short test beam periods these parameters could neither be optimized nor kept constant and the measured performance can be underestimated by about 15%.

Second, the CsI PC ageing caused by the ions bombardment from the avalanches inside a gaseous detector, requires a margin in the QE to ensure long-term PID performance in the validation criteria.

VIII. Module Commissioning in Test Beam

The commissioning in test beam is a fundamental step of the validation procedure both for the MWPC and for the PCs of each module. The MWPC is studied in terms of operation stability and gain uniformity, while the CsI PC QE is extracted from test beam data [9].

Module-1 has been equipped with old CsI PCs and tested in 2003. Module-2, Module-3 and Module-4 have been commissioned during summer '04 with final PCs (PC41 to PC57, Module-4 was missing one PC). Fig. 9 shows Module-3 at the CERN/SPS-X5 test beam, fully equipped with electronics. A typical event, produced by 120 GeV/c π^- is shown in Fig. 10; the grey-scale coding is proportional to the signal induced on the pads.

Given the relation between the Cherenkov angle resolution and the number of detected photons, it is of fundamental importance to locate correctly the single photoelectrons. The signal corresponding to a single photoelectron can be induced on one pad or on a group of adjacent pads (*cluster*). In addition, if detected Cherenkov photons hit the same pad or adjacent pads, the pad cluster will "include" more than one photon. Therefore, a simple *raw* cluster counting would result in a wrong measurement of the photoelectrons number and position.

Using a classification based on size, shape and pad pulse height (PH) distribution [9], some clusters are split into smaller so-called *resolved clusters* corresponding to single photoelectrons. If n local PH maxima are found in the original raw cluster,

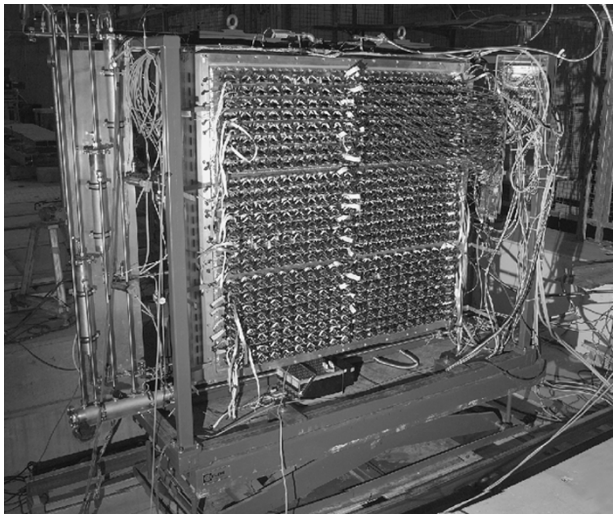

Fig. 9. A photo of Module-3 at the CERN/SPS-X5 test beam.

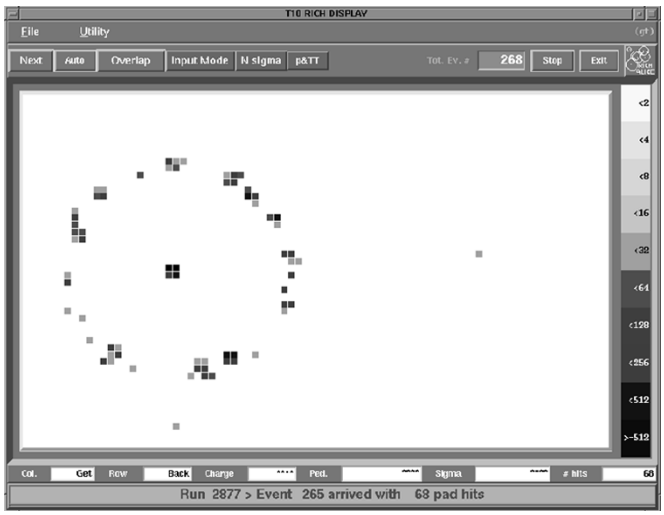

Fig. 10. An event produced by 120 GeV/c π^-. The display size is 80 × 48 pads, corresponding to one CsI PC.

n resolved clusters are created. The pads in the raw cluster are associated to a given resolved cluster depending on the closeness to the local PH maxima. If the pad is equidistant from two or more maxima, it is associated to all corresponding resolved clusters with a PH contribution weighed by the PH maxima. Then the photons position is estimated with the centroid calculation.

The number of resolved clusters represents the best estimation of the number of detected Cherenkov photons. The procedure is not fully efficient, since it has been found, by Monte Carlo simulation, that about 20% of *unresolved* clusters still contains the signal of more than one photoelectron.

Fig. 11 presents a graph of the number of the resolved clusters per event in PC45 as a function of the gas gain, for three MIP (minimum ionizing particle) positions. Gain variations of about 5% and PC response variations of about 10% are observed over the scanned area.

Fig. 12 shows the summary of the performance, i.e., average number of resolved clusters and corresponding Cherenkov angle

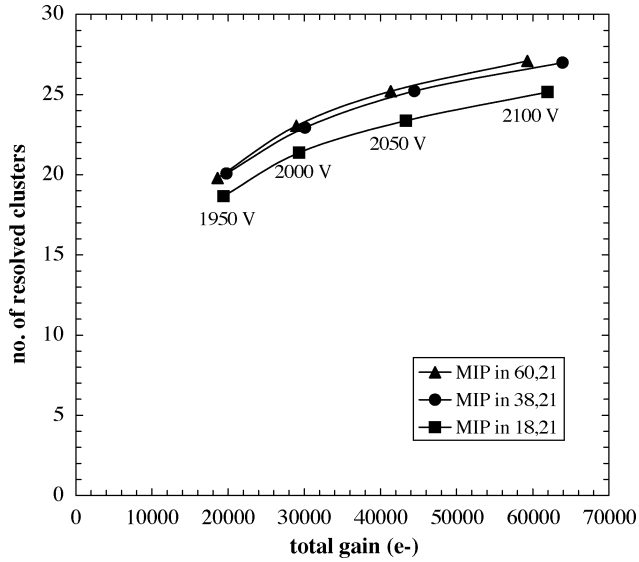

Fig. 11. The number of resolved clusters in PC45 as a function of the gas gain, in three MIP positions. The 10% decrease in the number of clusters observed in position 18,21 matches the response mapping shown in Fig. 6.

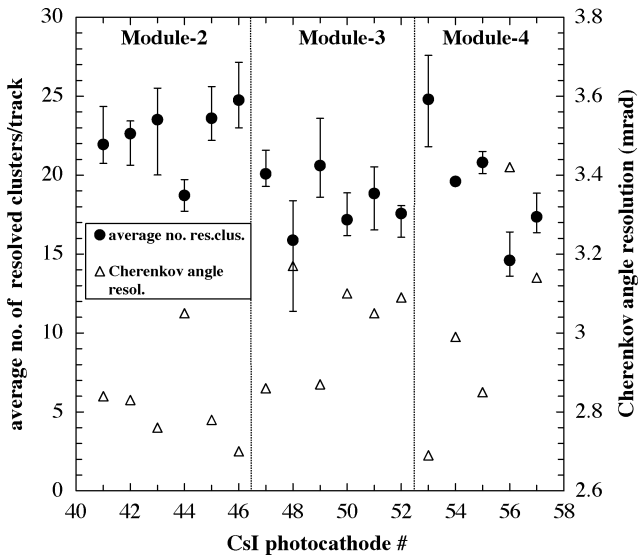

Fig. 12. The average number of resolved clusters and the corresponding Cherenkov angle resolution for each PC in Module-2, Module-3, and Module-4 at 2050 V. The error bars represent the spread in the number of clusters over the scanned PC area.

resolution, measured in each PC of Module-2, Module-3, and Module-4, at anode wires voltage of 2050 V.

The error bars represent the maximum and minimum number of resolved clusters over the PC scanned area. As mentioned in the previous section, variations in the number of clusters are determined not only by the QE of each PC but also by gas gain and C_6F_{14} transparency, which could not be kept constant during the full beam test of the three modules. In particular, the variations of the C_6F_{14} transmission (Fig. 13), caused by the unavoidable introduction of air in the circulation system at each module installation, resulted in fluctuations of the number of resolved clusters up to 15%. Applying the acceptance threshold of 17 resolved clusters, PC48 and PC56 have been rejected and will be re-coated after proper cleaning.

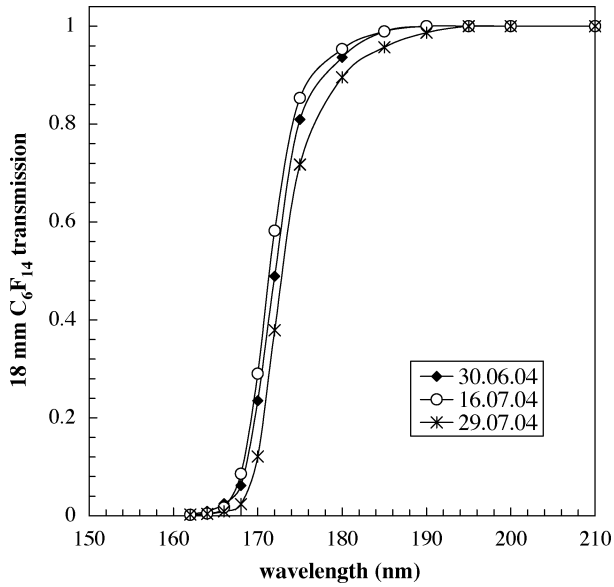

Fig. 13. The transmission of 18-mm-thick samples of C_6F_{14} in three different days during the test beam period of Module-2. The measurement is performed using a cell with calcium fluoride windows which can be attached to the circulation system, filled with C_6F_{14} and moved to the transmission measurement setup.

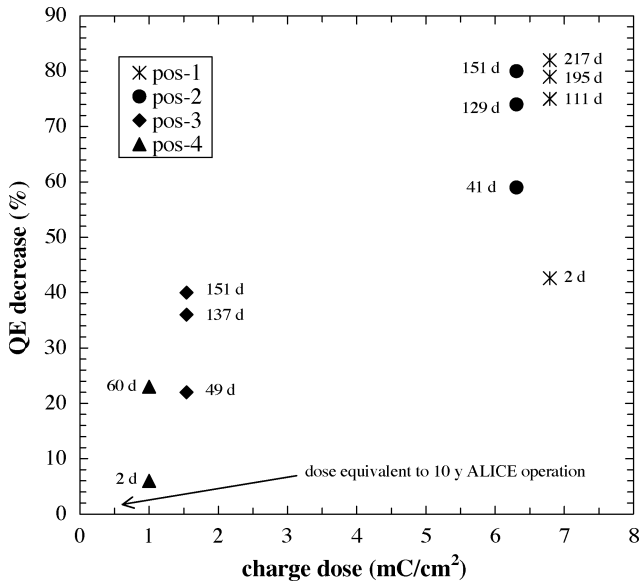

Fig. 14. The integral PC39 QE reduction as a function of the accumulated dose at different positions on the PC and its evolution in time (next to the symbols are shown the periods in days after the irradiation in which the PC has been measured in the VUV scanner). The HMPID detector expects 0.5 $\mathrm{mC/cm^2}$ in 10 years of operation in the ALICE experiment.

IX. CsI Ageing Studies

CsI ageing has to be taken into account in the PC validation for the mass production, in order to preserve the optimal PID performance during the 10 years operation of ALICE.

The long-term stability of CsI PCs kept under dry gas has been proven in the past [6], [11]. It is also well known that CsI ageing results from irradiation with very intense photon flux, larger than $10^{12}\ \mathrm{cm^{-2}s^{-1}}$ (far from our application), or from bombardment of the ions produced in avalanches, when operating in a gaseous detector [12]–[16].

Both processes are believed to cause a dissociation of the CsI molecules leading to an enrichment of Cs at the surface, with an increase of the electron affinity and a decrease of the QE.

The situation deduced from available literature data is rather puzzling, since ageing tests are performed on small CsI samples deposited on different substrates, exposed to air for the transfer between measurement setups and irradiated with quite large doses and rates, usually not corresponding to real operating conditions. In addition, the CsI QE decrease is measured only during the test (by the photocurrent decay) or verified by direct QE measurement, shortly after [15].

Trying to establish a methodological approach closer to realistic experimental detector operation, we performed several tests by irradiating with a collimated Sr-90 source a final size CsI PC (PC39) installed in a detector prototype operated with CH_4 [10], [17]. The accumulated charge, corresponding to the ions from the gaseous avalanches produced by the emitted βs, has been calculated from a direct measurement of the total current over the irradiated area of 4×5 pads.

Fig. 14 shows the PC39 QE decrease measured by the VUV scanner, in four different source locations and its evolution in time: the values next to the symbols represent the days after the completion of the irradiation. The most relevant aspect of these results, although preliminary, is the *self-ageing* of the irradiated areas, an effect reported only in [18]. After some time, the QE decrease seems to approach a saturation level depending on the charge dose, in absence of further irradiation. A scaling of the QE reduction for the dose of 0.5 $\mathrm{mC/cm^2}$, expected on the HMPID detector after 10 years operation of ALICE, should correspond to a final level of 10%–20%, which has been taken into account for the validation of the PCs. However, CsI PCs operated in a RICH prototype and exposed to smaller doses and irradiation rates, in beam tests and in the STAR experiment at BNL, have shown a remarkable stability with a response decrease not exceeding 5% over four years [19]. Clearly, to draw any conclusion, further tests are needed to study the observed self-ageing on a longer time-scale and at lower rates (the dose of 1 $\mathrm{mC/cm^2}$ was accumulated in about five days).

X. Conclusions and Outlook

Five out of seven modules of the ALICE HMPID detector, including the final FEE, have been assembled and commissioned in the laboratory and using a test beam.

The CsI PC mass production has started and the VUV scanner system for the PC characterization has been commissioned. Seventeen out of a total of 42 PCs have been produced and tested.

A beam test of three modules equipped with the final CsI PCs established the acceptance threshold for the serial production of all PCs. A maximum decrease of 20% in the QE after a 10-year operation has been deduced from preliminary results of the ageing tests; this result will be used in the validation criteria to assure good PID performance during the 10 years of operation of ALICE. According to the presently established acceptance threshold, 15 out of 17 produced PCs have been validated. Further tests will be performed to study the observed self-ageing on a longer time-scale and at lower charge rates.

The remaining modules will be equipped with final PCs and tested with cosmic rays before the installation in the ALICE magnet, starting in January 2006.

ACKNOWLEDGMENT

The authors gratefully acknowledge the excellent technical work of P. Ijzermans and J. Van Beelen and the contribution of C. David, D. Dell'Olio, L. Dell'Olio, D. Fraissard, Y. Lesenechal, L. Liberti, V. Rizzi, and M. Van Stenis. They would also like to thank W. Klempt for the valuable support to the project. Finally, the contribution of K. Kadija is also acknowledged.

REFERENCES

[1] ALICE collaboration, "ALICE physics performance report, volume 1," *J. Phys. G*, vol. 30, no. 11, p. 1517, Nov. 2004.

[2] "ALICE HMPID Tech. Des. Rep.,", CERN/LHCC 98/19.

[3] F. Piuz, Y. Andres, A. Braem, M. Davenport, A. Di Mauro, and A. Goret *et al.*, "The CsI-based ring imaging detector for the ALICE experiment: technical description of a large prototype," *Nucl. Instrum. Meth.*, vol. A433, p. 222, 1999.

[4] J. C. Santiard and K. Marent, "The Gassiplex0.7-2 integrated front-end analog processor for the HMPID and the dimuon spectrometer of ALICE," in *Proc. 5th Workshop Electronics for the LHC Experiments*, Snowmass, CO, Sep. 1999, p. 431.

[5] E. Nappi, "The CsI-RICH detector for high momentum hadron identification in the ALICE experiment at CERN-LHC," presented at the Proc. XLII Int. Winter Meeting Nuclear Physics, Bormio, Italy, Jan 25–31, 2004.

[6] A. Braem, M. Davenport, A. Di Mauro, P. Martinengo, E. Nappi, G. Paic, F. Piuz, and E. Schyns, "Aging of large area CsI photocathodes for the ALICE HMPID prototypes," *Nucl. Instrum Meth.*, vol. A515, p. 307, 2003.

[7] E. Schyns, "Status of large area CsI photocathode developments," *Nucl. Instrum. Meth.*, vol. A494, p. 441, 2002.

[8] A. Braem, C. Joram, F. Piuz, E. Schyns, and J. Séguinot, "Technology of photocathode production," *Nucl. Instrum. Meth.*, vol. A502, p. 205, 2003.

[9] A. Di Mauro, D. Cozza, M. Davenport, D. Di Bari, D. Elia, P. Martinengo, A. Morsch, E. Nappi, G. Paic, and F. Piuz, "Performance of large area CsI-RICH prototypes for ALICE at LHC," *Nucl. Instrum. Meth.*, vol. A433, p. 190, 1999.

[10] H. Hoedlmoser, "Quality-evaluation of CsI photocathodes for the ALICE/HMPID detector," presented at the RICH2004, 5th Int. Workshop Ring Imaging Cherenkov Counters, Playa del Carmen, Mexico, Nov. 30–Dec. 5 2004.

[11] A. Di Mauro, P. Martinengo, F. Piuz, E. Schyns, J. van Beelen, and T. D. Williams, "Study of the quantum efficiency of CsI photo-cathodes exposed to oxygen and water vapor," *Nucl. Instrum. Meth.*, vol. A461, p. 584, 2001.

[12] A. Breskin, "CsI UV photocathodes: history and mistery," *Nucl. Instrum. Meth.*, vol. A371, 1996.

[13] J. Va'vra, "Photon detectors with gaseous amplification," *Nucl. Instrum Meth.*, vol. A387, p. 137, 1997.

[14] J. Va'vra, A. Breskin, A. Buzulutskov, R. Chechik, and E. Shefer, "Study of CsI photocathodes: volume resistivity and ageing," *Nucl. Instrum. Meth.*, vol. A387, p. 154, 1997.

[15] B. K. Singh, E. Shefer, A. Breskin, R. Chechik, and N. Avraham, "CsBr and CsI UV photocathodes: new results on quantum efficiency and ageing," *Nucl. Instrum. Meth.*, vol. A387, p. 364, 2000.

[16] F. Piuz, "Ring imaging Cherenkov systems based on gaseous photo-detectors: trends and limits around particle accelerators," *Nucl. Instrum. Meth.*, vol. A502, p. 76, 2003.

[17] A. Braem, G. De Cataldo, M. Davenport, A. Di Mauro, A. Franco, A. Gallas, H. Hoedelmoser, P. Martinengo, E. Nappi, F. Piuz, and E. Schyns, "Results from the ageing studies of large CsI photocathodes exposed to ionizing radiation in a gaseous RICH detector," presented at the RICH2004, 5th Int. Workshop Ring Imaging Cherenkov Counters, Playa del Carmen, Mexico, Nov. 30–Dec. 5 2004.

[18] A. Breskin, A. Buzulutskov, R. Chechik, B. K. Singh, A. Bondar, and L. Shekthman, "Sealed GEM photomultiplier with a CsI photocathode: ion feedback and ageing," *Nucl. Instrum. Meth.*, vol. A478, p. 225, 2002.

[19] A. Braem, M. Davenport, A. Di Mauro, P. Martinengo, E. Nappi, G. Paic, F. Piuz, and E. Schyns, "Aging of large area CsI photocathodes for the ALICE HMPID prototypes," *Nucl. Instrum. Meth.*, vol. A515, p. 307, 2003.